*30th EPS Conference on Contr. Fusion and Plasma Phys., St. Petersburg, 7-11 July 2003 ECA Vol. **27A**, P-2.141*

Time–Frequency Analysis of Non-Stationary Signals in Fusion Plasmas Using the Choi-Williams Distribution

A.C.A. Figueiredo, M.F.F. Nave, and EFDA–JET contributors

Centro de Fusão Nuclear, Associação Euratom–IST, Instituto Superior Técnico, Lisboa, Portugal

Introduction

The Choi-Williams distribution is applied to the time–frequency analysis of signals describing rapid magnetohydrodynamic modes and events in tokamak plasmas. Its effectiveness is demonstrated through a comparison with the spectrogram, which requires a compromise between time and frequency resolution; and with the Wigner distribution, which can give an unclear representation of the modes, masked by inconvenient artifacts. Examples of phenomena in the JET tokamak are shown, namely the onset of neoclassical tearing modes in discharges with ion cyclotron resonant heating, precursors of edge localized modes, and washboard modes.

The spectrogram and the Choi-Williams distribution

The discrete-time spectrogram of a sampled signal $s(n)$ is the square of its short-time Fourier transform, that is, of the Fourier transform of the windowed signal $s(m)h(n-m)$ [1],

$$P(n,\theta)=\left|\frac{1}{\sqrt{2\pi}}\sum_{m=-\infty}^{+\infty}s(m)h(n-m)\exp(-i m\theta)\right|^2,$$

$n=t f_S$ and $\theta=2\pi f/f_S$ being the sample number and the normalized frequency, respectively, written in terms of time *t*, frequency *f*, and the sampling frequency f_S. The window $h(n)$ has length *l*, being zero except for $-(l-1)/2\le n\le+(l-1)/2$. The time resolution of the spectrogram is here calculated as half the duration of the chosen window, that is, $\delta t_P=(l-1)/(2f_S)$. Despite its widespread use, the spectrogram is notorious for implying a trade-off between time and frequency resolution [1]. Although the Wigner distribution [1, 2–4] overcomes this limitation, its application to signals with multiple components can be hindered by the presence of artifacts [5, 6], which are easily recognizable by their oscillatory nature [5]. The Choi-Williams distribution [7] is a so-called reduced interference distribution [5] that, by varying a parameter, gradually decreases the magnitude of artifacts as they are spread throughout the time–frequency plane. It allows signals with multiple components to be analysed with better resolution than the spectrogram, while reducing the artifacts in the Wigner distribution. The discrete form of the Choi-Williams distribution is [7]

$$CW(n,\theta;\sigma)=2\sum_{\tau,\mu=-\infty}^{+\infty}s(n+\mu+\tau)s^*(n+\mu-\tau)h_\tau(\tau)h_\mu(\mu)\exp(-i2\tau\theta)I(\mu,\tau;\sigma).$$

The parameter σ controls the level of artifacts and $h_\tau(n)$ and $h_\mu(n)$ are windows of length l_τ and l_μ, respectively. Unlike the spectrogram, windows play no fundamental role here, being required only because signals have limited durations, which implies that summations in τ and μ must be stopped somewhere. The function $I(\mu,\tau;\sigma)$ is given by

$$I(\mu,\tau;\sigma)=\frac{1}{2\pi}\int_{-\pi}^{+\pi}\exp\left(i\xi\mu-\frac{\xi^2\tau^2}{\sigma}\right)d\xi\approx\exp\left(-\frac{\mu^2}{4\tau^2}\sigma\right)\Big/2\sqrt{\frac{\pi}{\sigma}}|\tau|,$$

where it is assumed that $\exp(-\xi^2\tau^2/\sigma)$ is negligible for ξ outside the range $(-\pi,+\pi)$. Aliasing, which is intrinsic to $CW(n,\theta;\sigma)$ [7], can be avoided by replacing $s(n)$ with the corresponding analytic signal [1, 2–4, 7], making it possible to deal with frequencies up to $f_S/2$. For large σ values, $I(\mu,\tau;\sigma)$ approaches $\delta_{\mu,0}$. So, in the $\sigma\to\infty$ limit, $CW(n,\theta;\sigma)$ becomes the Wigner

distribution, with optimal time–frequency resolution. Decreasing σ leads to a reduction of artifacts, along with some loss of resolution due to the longer range of the summation in μ allowed by $I(\mu,\tau;\sigma)$. Still, such loss of resolution will not be significant provided σ is not made too low. Moreover, smearing in the time direction, due to the summation in μ, is effectively limited by the length of $h_\mu(n)$, since only samples symmetrically placed around each $n+\mu$, which is within a range $(l_\mu-1)/2$ of n, will be taken into account in the calculation of $CW(n,\theta;\sigma)$ at sample n. Notice that the summation in τ, symmetrical with respect to n, which exists in the Wigner distribution, implies no smearing at all — it in fact guarantees that the Wigner distribution is zero before a signal starts and after it ends [5]. So, the time resolution of $CW(n,\theta;\sigma)$ can be calculated as half the $h_\mu(n)$ window duration, that is, $\delta t_{CW}=(l_\mu-1)/(2f_S)$. This, however, is a maximum value for δt_{CW}. For large enough σ it is not the length of $h_\mu(n)$ that determines the resolution of $CW(n,\theta;\sigma)$, but the range within which $I(\mu,\tau;\sigma)$ significantly differs from zero.

Results

Given its good time–frequency resolution, the Choi-Williams distribution can identify fast precursors of magnetohydrodynamic (MHD) instabilities, such as edge localized modes (ELM), or resolve events occurring closely in time, such as the onset of neoclassical tearing modes (NTM) and sawtooth crashes, or the rapid interaction between ELM precursors and washboard (WB) modes. Here, all signals are from the JET tokamak and have been sampled at $f_S=250\,\text{kHz}$, a relatively low value in JET. A logarithmic scale is used in all time–frequency plots. Since the Choi-Williams distribution is negative in regions where artifacts exist [7], $\pm\log[\pm CW(n,\theta;\sigma)]$ is represented for $|CW(n,\theta;\sigma)|>1$, so that the argument of the logarithm is always positive. Spectrogram and $h_\tau(n)$ windows are of the Hanning type, while $h_\mu(n)$ windows are rectangular [1].

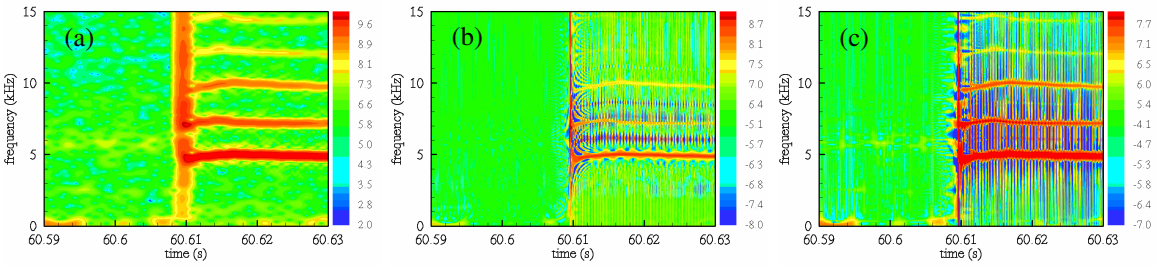

Figure 1. Analysis of a magnetic pick-up coil signal (JET pulse 50668), using (a) the spectrogram with l = 1023, (b) the Choi-Williams distribution with l_τ = 2047, l_μ = 63, and σ = 100, and (c) the Choi-Williams distribution with l_τ = 2047, l_μ = 511 and σ = 1. The (m=3, n=2) NTM, with a frequency of 5 kHz, appears simultaneously with the sawtooth crash at 60.6095 s.

Onset of NTM MHD mode analysis using techniques based on the short-time Fourier transform shows that, for JET pulses with large neutral beam injection (NBI) powers, the (m=3, n=2) NTM typically starts a few tenths of milliseconds before a sawtooth crash [8–10]. However, it has not been possible to resolve the time of the NTM onset with respect to the sawtooth in low β_N discharges with low NBI (less than 5 MW) and ion cyclotron resonance heating (ICRH), giving the impression that in these cases with low plasma rotation, the NTM started with, or after the sawtooth crash [9, 11]. A magnetic pickup-coil signal, containing information on a sawtooth crash occurring during the L-mode phase of a discharge with combined NBI and ICRH heating (P_{NBI} = 3MW plus P_{ICRH} = 1.5 MW), is here analysed with the spectrogram and the Choi-Williams distribution. The sawtooth period is 680 ms. In figure 1 the sawtooth crash appears as a broadband event at 60.6095 s, along with several MHD modes that show as different signal components. It is seen in figure 1(a) that for l = 1023 the spectrogram has a reasonable frequency resolution, which allows modes to be identified. On the other hand, the time resolution, $\delta t_P=2\,\text{ms}$, is not so good, causing the region around the crash to appear blurred. The crash and

the modes that show afterwards seem to appear at the same time. However, it is impossible to tell, with a time resolution better than 2 ms, if such modes appeared simultaneously with, shortly after, or already existed briefly before the sawtooth crash. Narrowing the window would improve the time resolution, but the inevitable broadening of the modes in the frequency direction would make them unrecognizable. Figure 1(b) depicts the Choi-Williams distribution for a high value of σ, that is, essentially the Wigner distribution. The time resolution, $\delta t_{CW} = 0.1\,\mathrm{ms}$, is considerably better than δt_P, the modes and the sawtooth crash being sharply represented. Looking at figure 1(b), it can be said, with much greater certainty than with the spectrogram, that the (m=3, n=2) NTM, which appears at 5 kHz, starts simultaneously with the sawtooth. In addition, unlike the higher β_N, NBI heated pulses [8-10], no growing sawtooth precursor can be identified before the crash. Artifacts appearing in-between every pair of signal components make the picture unclear in some places, some of those artifacts being superposed on the higher-frequency modes. Since the magnitude of artifacts is proportional to the product of the interfering components [5, 7], lower-amplitude modes may be masked by artifacts that result from the interference of such modes with the higher-amplitude ones, which explains why the higher-frequency modes, with lower amplitudes, are less visible. The result of using a lower σ is seen in figure 1(c), where the higher-frequency modes can now be clearly seen, thanks to the reduction of artifacts, although now the time resolution is only $\delta t_{CW} = 1\,\mathrm{ms}$ because a longer $h_\mu(n)$ window has been used.

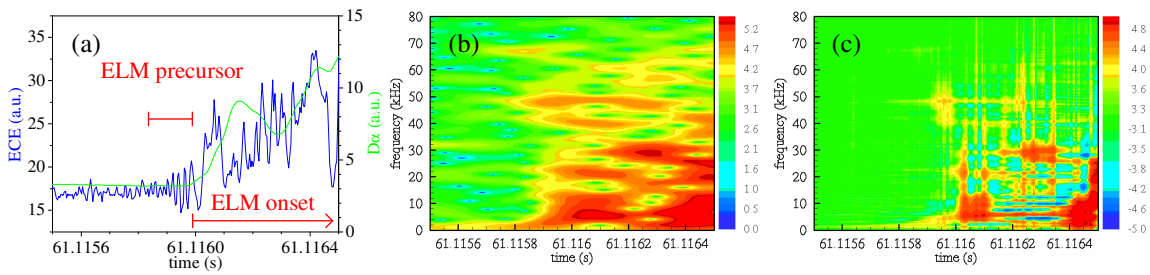

Figure 2. In (a) edge ECE and Dα signals (JET pulse 53060) reveal the presence of an ELM precursor between 61.1158 s and 61.1160 s, with a frequency of about 50 kHz. The ECE signal has been analysed using (b) the spectrogram with l = 127, and (c) the Choi-Williams distribution with l_τ = 4095, l_μ = 63 and σ = 1.

ELM precursors Figure 2(a) shows an electron cyclotron emission (ECE) signal in which, in conjunction with the Dα signal that is also shown, it is possible to identify an ELM precursor [12] with frequency around 50 kHz. As the precursor only lasts about 0.2 ms, the spectrogram in unable to resolve it. As seen in figure 2(b), done with a time resolution of $\delta t_P = 0.25\,\mathrm{ms}$, just about the expected duration of the precursor, the frequency resolution of the spectrogram is already insufficient to yield a clear picture. The result of applying the Choi-Williams distribution to this signal can be seen in figure 2(c). The time resolution is $\delta t_{CW} = 0.1\,\mathrm{ms}$. The precursor is clearly shown at 50 kHz, and other low frequency modes that exist in the signal can be seen as well.

Washboard modes WB modes have been seen to interact with ELM precursors, in a way suggesting that both phenomena cannot happen at the same time [13, 14]. Time–frequency mode-number plots, which, like the spectrogram, are based on short-time Fourier analysis, have been presented to demonstrate this behaviour [13, 14]. In such plots, WB modes are seen as several broad frequency bands of magnetic fluctuations, not having well-defined frequencies. Here, a magnetic signal is analysed where it is possible to see this interaction between a type-I ELM precursor at 15 kHz and WB modes between 25

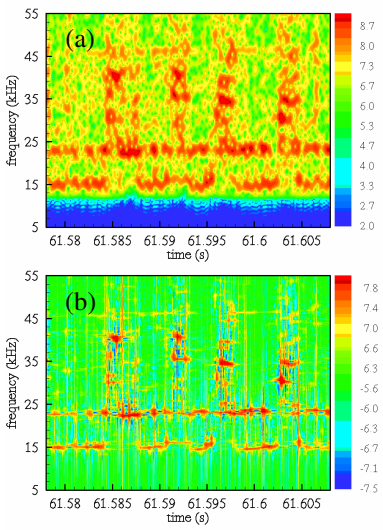

Figure 3. Analysis of a magnetic pick-up coil signal (JET pulse 55976), using (a) the spectrogram with l = 255, and (b) the Choi-Williams distribution with l_τ = 2047, l_μ = 255, and σ = 0.5. The interruption of the WB modes by the type-I ELM precursor is best seen with the Choi-Williams distribution.

kHz and 50 kHz [13, 14]. Signal components below 13 kHz have been removed by filtering to provide clearer pictures. Figure 3(a) shows a spectrogram with time resolution $\delta t_P = 0.5\,\mathrm{ms}$, which allows seeing the intermittent ELM precursors and WB modes. Although the alternating appearance of the two mode types can be seen with the spectrogram, the trade-off between time and frequency resolution limits the sharpness of the time–frequency representation. A clearer time–frequency picture is achieved with the Choi–Williams distribution, as shown in figure 3(b), where a better frequency resolution is achieved with the same time resolution of the above spectrogram, $\delta t_{CW} = 0.5\,\mathrm{ms}$.

Conclusions

The Choi-Williams distribution has been used to process fusion plasma signals that have also been analysed using the spectrogram and the Wigner distribution. Adequate time resolution, with suitable reduction of artifacts, has been obtained for such signals by judiciously choosing σ and the length of the used windows. The conclusion, with a much smaller time uncertainty than with the spectrogram, that the (m=3, n=2) NTM occurs simultaneously with the onset of a sawtooth crash in a low β_N discharge, was only possible given the high time–frequency resolution and low level of artifacts of the Choi-Williams distribution. It was also possible to visualize a short ELM precursor in the time–frequency plane, and to provide a picture of the interaction between ELM precursors and WB modes that is much clearer than those produced with the spectrogram. So, the Choi-Williams distribution can offer an improved time–frequency view of some types of events, provided σ and the length of windows can be chosen to avoid masking of signal components by artifacts.

Acknowledgments

We are thankful to S. Pinches and C. Perez for useful discussions and suggestions. This work, which has been supported by the European Communities and the Instituto Superior Técnico (IST) under the Contract of Association between the European Atomic Energy Community and IST, has been carried out within the framework of the European Fusion Development Agreement. Financial support has also been received from the Fundação para a Ciência e Tecnologia (FCT) in the frame of the Contract of Associated Laboratory. The views and opinions expressed herein do not necessarily reflect those of the European Commission, IST or FCT.

References

[1] Bizarro J.P.S. and Figueiredo A.C. 1999 *Nucl. Fusion* **39** 61, 697
[2] Claasen T.A.C.M. and Mecklenbräuker W.F.G. 1980 *Philips J. Res.* **35** 217
[3] Claasen T.A.C.M. and Mecklenbräuker W.F.G. 1980 *Philips J. Res.* **35** 276
[4] Claasen T.A.C.M. and Mecklenbräuker W.F.G. 1980 *Philips J. Res.* **35** 372
[5] Cohen L. 1995 *Time–Frequency Analysis* (Englewood Cliffs, NJ: Prentice-Hall)
[6] Figueiredo A.C.A. and Bizarro J.P.S. 2002 *IEEE Trans. Plasma Sci.* **30** 54
[7] Choi H. and Williams W.J. 1989 *IEEE Trans. Acoust., Speech, Signal Process.* **37** 862
[8] Nave M.F.F. *et al* 2003 *Nucl. Fusion* **43** 179
[9] Belo P. *et al* 2001 *Proc. 28th EPS Conf. on Control. Fusion and Plasma Phys. (Madeira, Portugal)* vol 25A (ECA), p 1785
[10] Buttery R. *et al* 1999 *Proc. 26th EPS Conf. on Control. Fusion and Plasma Phys. (Maastricht, Netherlands)* vol 23J (ECA), p 121
[11] Sauter O. *et al* 2001 *Proc. 28th EPS Conf. on Control. Fusion and Plasma Phys. (Madeira, Portugal)* vol 25A (ECA), p 449
[12] Perez C.P. *et al* 2002 "Type-I ELM Precursor Modes in JET", submitted to *Nucl. Fusion*
[13] Perez C.P. *et al* 2003 "Washboard modes as ELM-related events in JET", submitted to *Plasma Phys. Control. Fusion*
[14] Koslowski H.R. *et al* 2003 "Relation between type-II ELMs, edge localised turbulence, washboard modes and energy losses between ELMs in high density ELMy H-modes on JET", *this conference*